Biosensors and Bioelectronics 55 (2014) 187–194

Contents lists available at ScienceDirect

Biosensors and Bioelectronics

journal homepage: www.elsevier.com/locate/bios

Intra-molecular G-quadruplex structure generated by DNA-templated click chemistry: "Turn-on" fluorescent probe for copper ions

Qinpeng Shen [a,b], Lifen Zhou [a], Yijia Yuan [a], Yan Huang [a,*], Binbin Xiang [a], Chunyan Chen [a], Zhou Nie [a,*], Shouzhuo Yao [a]

[a] State Key Laboratory of Chemo/Biosensing and Chemometrics, College of Chemistry and Chemical Engineering, Hunan University, Changsha 410082, PR China

[b] Yunnan Academy of Tobacco Science, Kunming 650106, PR China

ARTICLE INFO

Article history:
Received 8 October 2013
Received in revised form
5 December 2013
Accepted 6 December 2013
Available online 16 December 2013

Keywords:
G-quadruplex
DNA-templated organic synthesis (DTS)
Click chemistry
Copper ion
Crystal violet (CV)

ABSTRACT

A novel homogenous fluorescent sensor for signal-on detection of Cu^{2+} has been developed based on intra-molecular G-quadruplex formed by DNA-templated click reaction and crystal violet (CV) as label-free signal reporter. The clickable DNA probe consists of two G-rich strands (A and B) bearing azide and alkyne group, respectively, and a template strand (C) locating two proximate reactants by pairing with A and B. The sequences of A and B are derived from asymmetric split of the G-quadruplex sequence $(TTAGGG)_4$. In the presence of Cu^{2+}, the whole G-quadruplex sequence A–B is generated by chemical ligation of A and B via copper ion-catalyzed alkyne-azide cycloaddition, then released from template by toehold strand displacement, and consequently forming a stable intra-molecular G-quadruplex, which binds with CV to generate a strong fluorescent signal. Oppositely, weak fluorescence was obtained without Cu^{2+} because of unstable intermolecular G-quadruplex formed by A and B and lack of lateral loop connection. Therefore, the Cu^{2+} can be sensitively and specifically detected by the fluorescence of the CV-stained G-quadruplex with a low detection limit of 65 nM and a linear range of 0.1–3 μM. This method rationally integrated the DNA-templated synthesis and G-quadruplex structure-switch, presenting a simple and promising approach for biosensor development.

1. Introduction

G-quadruplexes are highly ordered nucleic acid structures composed by staked arrays of G-quartets (Phan et al., 2006). These structures have received constant attention due to not only their unique structure features but also their biological significance in telomere maintenance, transcription regulation and anti-tumor chemotherapy (Arthanari and Bolton, 2001; Hurley, 2002; Mergny et al., 2002; Neidle and Parkinson, 2003; Sen and Gilbert, 1990). G-quadruplexes are intriguing for their conformational polymorphism, which is dependent on several factors including base sequence, loop connectivity, and intercalated cation. Recently, some small fluorogenic molecules (such as triphenylmethane and protoporphyrin dyes) have been demonstrated to selectively bind G-quadruplexes and generate a strong fluorescence enhancement (Bhasikuttan et al., 2007; Kong et al., 2009a, 2009b; Li et al., 2010). Hence, several fluorescent methods have been developed to detect various analytes relied on the generation of fluorescent signal caused by such G-quadruplex-specific dyes binding with G-quadruplex. For example, Leung's group reported a simple and convenient G-quadruplex-based fluorescence detection method for $3'\rightarrow5'$ exonuclease activity using crystal violet (CV) as a G-quadruplex-binding probe (Leung et al., 2011). Wang's group exploited a turn-on fluorescent Pb^{2+} sensor based on Pb^{2+}-induced formation of G-quadruplex and zinc protoporphyrin dye (Li et al., 2010). These dyes are also fluorescently sensitive to conformation changes of G-quadruplex, which has been expanded to probe structure-switch of G-quadruplex induced by sequence change and intercalated ions. Kong's group employed two triphenylmethane dyes (CV and malachite green) to discriminate G-quadruplexes from duplex and single-stranded DNAs (Kong et al., 2009a). They also developed a CV-based fluorescent biosensor for the discrimination of parallel from antiparallel structure of G-quadruplexe and for monitoring the structural variation of G-quadruplexes (Kong et al., 2009b).

DNA-templated organic synthesis (DTS) is emerging as a powerful technique to drastically accelerate reaction rate and enhance reaction specificity owing to significant increase of reactants effective molarity through DNA-encoded small molecule

* Corresponding authors: Tel.: +86 731 8882 1626; fax: +86 731 8882 1848.
E-mail addresses: yanhuang.hnu@gmail.com (Y. Huang), niezhou.hnu@gmail.com (Z. Nie).

0956-5663/$ - see front matter © 2013 Elsevier B.V. All rights reserved.
http://dx.doi.org/10.1016/j.bios.2013.12.019

and base pairing-mediated proximity (Gartner et al., 2004; Li and Liu, 2004; Shen et al., 2012, 2013). With the aid of DTS, the non-natural organic reaction can be recognized, programmed, selected and amplified by DNA-related technology (Kanan et al., 2004). Its potent synthetic capabilities of DTS has also played an important role in various chemical and biological applications, including sequence-specific DNA modification, the creation and evaluation of libraries of synthetic molecules, homogenous peptide synthesis, bioactive molecule screening, biosensing and biolabeling (Doyon et al., 2003; Gartner et al., 2002; Halpin and Harbury, 2004; Kleiner et al., 2011; Tse et al., 2008). Moreover, the DTS-caused DNA chemical ligation provides an innovative tool to study the higher-order nucleic acid structures. Recently, DTS has been carried out to investigate G-quadruplex structures. Komiyama's group developed a method for probing G-quadruplex structures based on DTS-based chemical ligation (Xu et al., 2009). However, the application of DTS in the G-quadruplex-related biosensing is still largely unexplored.

Herein, we report a novel fluorescent biosensing strategy based on the DTS-induced generation of intra-molecular G-quadruplex structure. Crystal violet (CV) is chosen as a signal reporter since its fluorescence can be enhanced greatly via binding to G-quadruplex (Kong et al., 2009a, 2009b). Inspired by CV's fluorogenic property susceptible to G-quadruplex structure switch (Kong et al., 2009a, 2009b), we exploited CV to identify the integration of split-G quadruplex by DTS-caused chemical DNA ligation. Copper(I)-catalyzed alkyne-azide Huisgen cycloaddition (CuAAC), the well-known representative of “click chemistry”, was used as a linking tool for DNA chemical ligation owing to its high yield under moderate conditions and high specificity to the catalysis of copper(I) (Deiters et al., 2003; Rostovtsev et al., 2002; Wang et al., 2003). Copper ion is the third most abundant transition metal in humans and plays vital role in energy generation, dioxygen transport and activation, and signal transduction at physiological level (Que et al., 2008). On the contrary, high-level copper is highly toxic and pathogenic to living organisms (Georgopoulos et al., 2001). In this regard, it is significant to develop robust detection methods for copper ion in biological and environmental analysis. CuAAC has been emerged in copper ion sensing because of its superb specificity. First instance was reported by Hulme's group using CuAAC-induced generation of the sensitized Eu^{3+} complex to detect copper ion (Viguier and Hulme, 2006). Jiang's group developed a copper ion assay based on the CuAAC-mediated gold nanoparticles aggregation (Zhou et al., 2008). Afterwards, applying CuAAC to chemically link two organic motifs or nano-materials, several colorimetric and fluorescent Cu^{2+} assays have been developed (Hua et al., 2012; Song et al., 2010; Sanji et al., 2011). However, these early works were based on conventional organic reactions, leading to high concentrations of reactants required for the click reaction, long reaction time or relatively high detection limit. Recent efforts have been contributed to overcome these shortcomings by introduction of enzyme or nanoparticles-involved signal amplification approaches into CuAAC-based assays (Qiu et al., 2011; Su et al., 2013). Another effective strategy which can circumvent these disadvantages is to exploit highly efficient DTS instead of conventional CuAAC reaction. A colorimetric Cu^{2+} sensor via DTS-induced cross-linking aggregation of gold nanoparticles (AuNPs) was reported by Mirkin's group (Xu et al., 2010). Recently, we have developed a fluorescent copper ion biosensor via DNA-templated CuAAC and magnetic separation (Shen et al., 2012). These DTS-based assays achieved remarkably shorter reaction time, high sensitivity and good selectivity. Nevertheless, the detection process is relative tedious since alternating temperature and separation in the experimental process are required in current designs. Herein, the mix-and-read detection avoiding the thermal treatment and separation was achieved using the present homogeneous method, which can significantly simplify the process of DTS-based bioassays.

2. Experimental methods

2.1. Materials and measurements

Tris-(hydroxypropyltriazolylmethyl)amine (THPTA) was synthesized according to published literature (Chan et al., 2004; Liu et al., 2007). Tetrakis (acetonitrile) copper(I) hexafluorophosphate, tripropargylamine and 3-bromo-1-propanol were purchased from Sigma-Aldrich Chemical Co., (St, Louis, MO, USA). $CuSO_4 \cdot 5H_2O$, sodium ascorbate and sodium azide were purchased from BBI (Ontario, Canada). Crystal violet (CV) was obtained from Alfa (Ward Hill, MA, USA). Glutathione (GSH) was obtained from Sangon (Shanghai, China). All other chemical reagents were of analytical grade and obtained from Sinopharm Chemical Reagent Co., Ltd. (Beijing, China) and used without further purification. All the oligonucleotides used in this work were synthesized by Takara (Dalian, China). All solutions were prepared with ultra-pure water (18.25 MΩ cm) from a Millipore system. Fluorescence spectra were obtained on a PTI QuantaMasterTM 4 fluorescence spectrometer (Birmingham, NJ, USA). UV/Vis absorption spectra were obtained at 25 °C on a Beckman DU-800 spectrophotometer and the concentrations of oligonucleotides were determined by measuring the absorbance at 260 nm. CD spectra were measured on a Jasco J-715 spectropolarimeter at room temperature. The gels were visualized via fluorescence detection using a ChemiDoc MP system (Bio-Rad, USA). The sequences of these oligonucleotides are as follows:

A: 5′-TGCATTTAGGGTTA-azide-3′
B: 5′-alkyne-GGGTTAGGGTTAGGG-3′
C:5′-CCCTAACCCTAACCCTAACCCTAAATGCAAAAGAGCTCAGC-3′
D: 5′-GCTGAGCTCTTTTGCATTTAGGGTTAGGGTTAGGGTTA-3′
A-(PEG_{12})-B: 5′-TGCATTTAGGGTTA-(PEG_{12})-GGGTTAGGGTTAGGG-3′

2.2. Denaturing PAGE analysis of click ligation of oligonucleotides

Three single-stranded DNA A, B and C (2 μM), NaCl (100 mM), THPTA (1 mM) and sodium ascorbate (500 μM) were added to 4 μL of Tris–HCl buffer (20 mM Tris, pH=7.4) sequentially. Then 1 μL solution of Cu^{2+} with different concentration was added, and the reaction mixture was incubated at room temperature for 90 min. The other control experiments were conducted as the above procedure, except for adding different DNA to the reaction solution. The reaction mixture was then diluted into 1 × PAGE loading buffer containing 7 M urea. The reaction mixture was separated by denaturing PAGE on a 15% TBE/urea polyacrylamide gel. The electrophoresis was carried in 1 × tris-borate-EDTA (TBE) buffer (90 mM Tris, 90 mM boric acid, and 10 mM EDTA, pH 8.0) at 80 V for 3 h. After electrophoresis, the gels were stained by SYBR Green II.

2.3. Circular dichroism (CD) experiment

Oligonucleotide solutions (3 μM) were dissolved in 20 mM Tris–HCl buffer (pH 7.4) containing 100 mM NaCl and 20 mM KCl. To ensure the formation of G-quadruplex structures, the oligonucleotide solutions were heated to 90 °C for 5 min, cooled to room temperature, and then incubated at room temperature overnight for CD spectra analysis. CD spectra were measured in the range from 200 nm to 320 nm in 1 mm path length cuvettes.

CD spectra were averaged from 3 scans, which were recorded at 50 nm min^{-1} with a response time of 1 s and a bandwidth of 0.2 nm.

2.4. Typical experimental process for Cu^{2+} detection

Three single-stranded DNA A, B and C (2 μM), NaCl (100 mM), THPTA (1 mM) and sodium ascorbate (500 μM) were added to 40.0 μL of Tris–HCl buffer (20 mM Tris, pH = 7.4) sequentially. Then 10 μL solution of Cu^{2+} with different concentrations was added, and the reaction mixture was incubated at room temperature for 90 min. After incubation, ssDNA D (2 μM) was added to the resulting solution for sequential strand displacement, and the mixture was incubated at room temperature for 30 min. Then KCl (20 mM) and crystal violet (CV, 2 μM) were added to Tris–HCl buffer (20 mM Tris, pH = 7.4) sequentially, and the total volume was 100 μL. The reaction mixture was incubated at room temperature for 60 min. The fluorescence was then measured with PTI QuantaMasterTM 4 fluorescence spectrometer. The excitation wavelength was 580 nm, and the emission wavelengths were in the range from 600–680 nm with both excitation and emission slits of 5 nm.

3. Results and discussion

3.1. Principle for the biosensing system

The mechanism of our strategy is shown in Fig. 1A. The click reaction probe consists of three strands to form DTS template. Two G-rich strands (A and B) bearing azide group and alkyne group, respectively, were aligned together by their complementary strand C to bring their reactive groups into close proximity to one another. The sequence design of A and B was derived from the four repeated human telomere sequence $(TTAGGG)_4$, a typical intra-molecular G-quadruplex-forming sequence which has been proved to enhance CV fluorescence via binding with CV. Because of high symmetry of the 24 nt sequence, the identical sequence of A and B will be obtained if the 24 nt sequence is split equally. Thus, the hybridization of A and B with C provides four possible structure arrangements: one with two proximate labeled reactants, another with two reactants separated from each other and the other two with only one reactant (Fig. S1), which is undesirable for highly efficient DTS reaction. Based on above consideration, the asymmetric design was applied to ensure the only structure arrangement to locate two reactants proximate and head-to-head (detailed sequence profile of the probe is depicted in Fig. 1B). The 24 nt sequence was split into two parts of 9 nt and 15 nt (yellow parts), which were distributed to the sequences of partial A and whole B, respectively. To further increase the sequence specificity, additional 5 nt (red part) was included in the sequence A. Strand C, the template for DTS reaction, includes the complementary sequence of A and B as well as an additional 12 nt "toehold" domain which is used to remove C from A and B, once DTS is complete, via toehold displacement by a "remover" DNA D. Strand D contains complementary sequence to C but eliminates the 3 nt GGG at 3′ end, in order to fulfill the complete strand displacement and, moreover, avoid the potential interference of excess D bound with CV. With the introduction of Cu^{2+}, Cu^{+} is yielded via the reduction of Cu^{2+} by sodium ascorbate

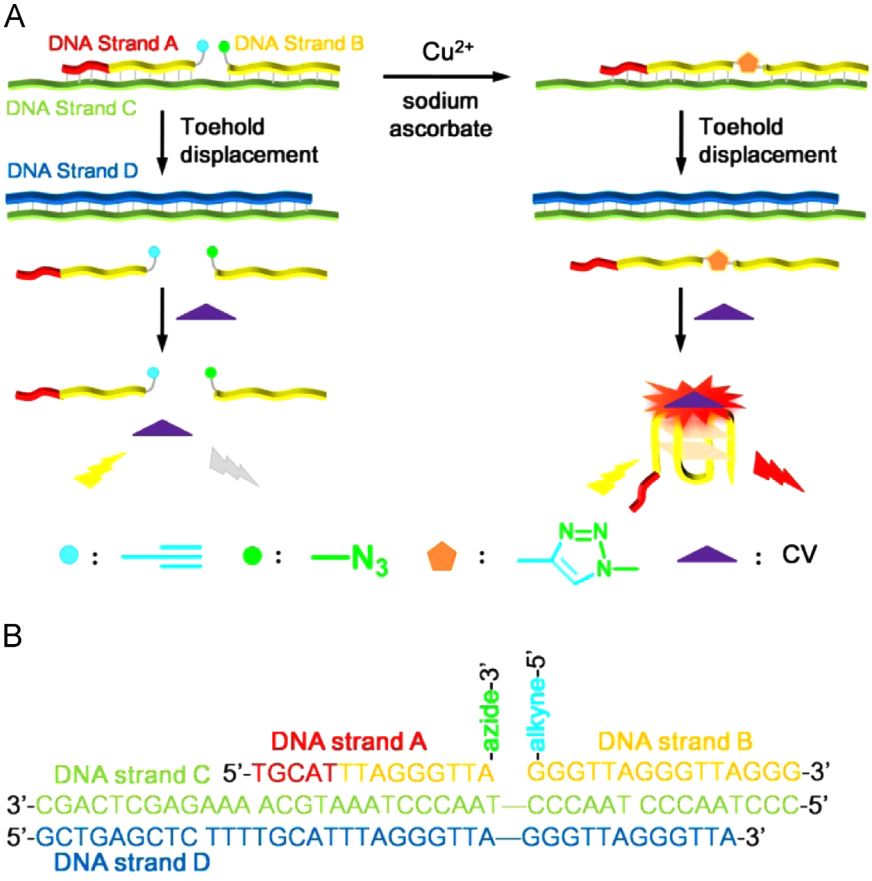

Fig. 1. (A) Schematic representation of DTS-induced generation of intra-molecular G-quadruplex for fluorescent detection of Cu^{2+}. (B) Detailed sequence profile of the probe. A stable helix formed by DNA strand A, B and C was used as DTS template. Strand D was used to initiate toehold displacement and remove C from A and B. (For interpretation of the references to color in this figure legend, the reader is referred to the web version of this article.)

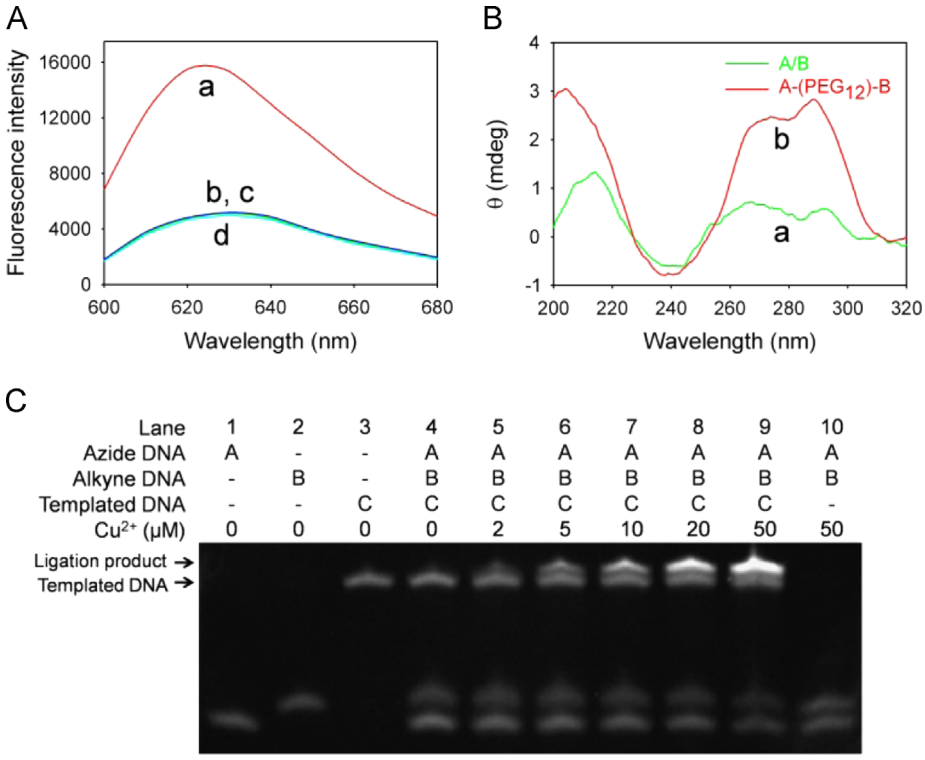

Fig. 2. Fluorescent detection of Cu^{2+}. (A) Fluorescence spectra of the CV stained DNA probe with treatment of 500 μM Na-Asc and 50 μM Cu^{2+} mixture (a), 500 μM Na-Asc (b), 50 μM Cu^{2+} (c) and without template DNA C (d). (B) CD spectrum of A/B mixture (a) and A-(PEG_{12})–B (b). (C) Product analysis of click reaction at room temperature for 90 min by denaturing PAGE.

(Na-Asc) and catalyzes the DNA-templated CuAAC to chemically ligate A and B. After click reaction, the "remover" strand D was added to initiate toehold-displacement. The newly formed A-B single-stranded DNA (ssDNA) was released and formed a stable intra-molecular G-quadruplex in the presence of K^+, which binds with CV to generate a strong fluorescent signal. In contrast, no chemical ligation occurs without Cu^{2+} and the strand displacement leads to the release of A and B. Since the G-quadruplex formed by A and B was unstable and lacked the loop connection between A and B, a weak fluorescent signal of CV was obtained. Thus, the copper ion can be quantitatively measured by the fluorescence of the CV-stained intra-molecular G-quadruplex formed by DTS and DNA strand displacement.

3.2. *Fluorescent biosensing of Cu^{2+}*

Fig. 2A shows a typical fluorescent detection of the Cu^{2+}. After addition of Cu^{2+}, click ligation of A and B occurs in the presence of the template strand C, excess Na-Asc and an accelerating Cu^+-binding ligand (THPTA). The click reaction mixture was incubated at room temperature for 90 min. Afterwards, strand D hybridizes with unpaired toehold of C to initiate strand displacement of A and B. After toehold-displacement, a very strong fluorescence emission at 630 nm was obtained by CV stain using K^+-caused G-quadruplex stabilization (spectrum a), indicating the formation of stable intra-molecular G-quadruplex by ligation product A–B. However, the control without Cu^{2+} (spectrum b) or Na-Asc (spectrum c) causes the weak fluorescence, implying that this click ligation is derived from reduction of Cu^{2+} by Na-Asc. The negligible fluorescence signal (spectrum d) compared with the background (spectrum b) was observed in the absence of template C, evidencing the extremely low efficiency of conventional CuAAC reaction at micromolar level of reactants without DNA template-directed reactant proximity and demonstrating the potency of DTS (Kumar et al., 2007).

To rationalize this Cu^{2+}-caused CV fluorescence enhancement, circular dichroism (CD) experiment was conducted to assess the supposed DTS-caused G-quadruplex structure switch. The detection system is the mixture of double-stranded DNA and G-quadruplex, which is unfavorable for CD measurement. Thus we used the A-(PEG_{12})-B, a complex of A and B (A/B) connected by PEG linker to mimic the click ligation product A–B. Both A-(PEG_{12})-B and the mixture of A and B show two positive bands at 290 nm and 264 nm and a negative band at 240 nm, a signature of mixed type G-quadruplex (the supposed G-quadruplex structures formed by various samples are shown in Fig. S2), (Karsisiotis et al., 2011) but the CD signal intensity of A-(PEG_{12})–B was much stronger than that of the A/B mixture (Fig. 2B). This demonstrated that the ligation product A–B is more preferable for G-quadruplex formation than A/B mixture. Moreover, the unconnected lateral loop in A/B intermolecular mixed-type G-quadruplex was another plausible reason for low fluorescence because this loop is crucial for CV fluorescence enhancement (Kong et al., 2009b). Herein, this Cu^{2+}-caused signal-on was attributed to the stable G-quadruplex formed by A–B and loop association by DTS.

To further verify the feasibility of the proposed method, some crucial issues were investigated. Neocuproine, a specific Cu^+ chelator, was used to confirm the generation of Cu^+ in click reaction solution due to the fact that neocuproine can react with Cu^+ to form a yellow complex with strong absorbance at 450 nm (Byrnes et al., 1992). As shown in Fig. S3, the sample with Cu^{2+} and Na-Asc changed from light blue to deep yellow as soon as neocuproine was added, while that with Cu^{2+} or Na-Asc only remained light blue. Correspondingly, a significant absorbance increase at 450 nm was recorded with the introduction of Cu^{2+} and Na-Asc. These results certify that Cu^+ was yielded in click reaction solution.

Denaturing polyacrylamide gel electrophoresis (PAGE) was employed to verify the ligation product of DTS. The click reaction was performed with probe hybrid A/B/C for 90 min at room

temperature and the resulting product was analyzed by denaturing PAGE. Fig. 2C shows that no reaction occurred without Cu^{2+} (lane 1 to 4). After addition of Cu^{2+}, a new band appeared and its mobility was comparable with that of C but remarkably slower than that of A or B (lane 5), indicating the yield of ligation product A–B. This product band became gradually brighter with increasing Cu^{2+} concentrations from 2 μM to 50 μM, revealing the copper ion dose-dependent manner of the click ligation (lane 5 to 9). Similar to the fluorescence result, the function of DTS was also demonstrated by no ligation product band in gel (lane 10) without the template strand C on account of low effective molarity of reactants without hybridization (Kumar et al., 2007).

The water-soluble tris-triazolylamine Cu^{+}-binding ligand (THPTA) was exploited here as a protector of DNA against Cu^{2+}-induced oxidative degradation (Kumar et al., 2007). Fig. S4A depicts the gel analysis concerning the protection role of THPTA. In the absence of THPTA, little ligation product was observed and extensive degradation of all DNA occurred because of oxidative damage induced by Cu^{2+} and Na-Asc. When greater than 5-fold excess of THPTA relative to the concentration of copper ion was introduced, very little decomposition of DNA was observed. Correspondingly, the biosensor without THPTA showed only a half fluorescence signal to 200 μM Cu^{2+} compared to that with THPTA (Fig. S4B). The denaturing PAGE and fluorescence experiment results confirm that THPTA can effectively protect DNA from oxidative damage. Thereby, 1 mM THPTA was introduced into the click reaction experiment.

3.3. Sensor optimization

Considering that the azide-alkyne click reaction is a major component of this copper ion biosensor, some influential factors of the click reaction were optimized firstly. Since the yield of click ligation was determined directly by the time of click reaction, the effect of click reaction time on the sensor response was investigated. The fluorescence signal of the proposed biosensor refers to the ratio (F/F_0) of fluorescence intensity at 630 nm with Cu^{2+} to that without Cu^{2+}. As shown in Fig. S5, the fluorescence signal increased with the increasing time from 0 min to 90 min and reached a plateau at 90 min. Thus 90 min was chosen as the time of click reaction in following experiments, which is much shorter than that used in some previous assays based on conventional organic click reactions (Song et al., 2010; Sanji et al., 2011; Zhou et al., 2008). This might be attributed to that the DNA template-mediated reactant proximity can accelerate the reaction rate of CuAAC (Gartner et al., 2004; Li and Liu, 2004; Shen et al., 2012, 2013).

The temperature of click reaction, another potential factor influencing the reaction efficiency, was optimized by conducting the click reaction at different temperature ranging from 4 °C to 40 °C. As depicted in Fig. S6, the fluorescence signal ratio (F/F_0) is not significantly affected by temperature. In order to facilitate the experimental operation, all the click reactions in this study were incubated at room temperature.

The solution pH is also an important parameter for the copper (I)-catalyzed click chemistry. Fig. S7 exhibits the effect of varying pH (4–12) on click reaction. The sensor displayed maximal signal when click reaction was conducted in neutral or weak alkaline solution (pH from 7 to 10). In the acidic conditions (pH < 7), Cu^{+} is prone to give disproportionation reaction and yields Cu^{2+} and zero-valent copper (Barceloux, 1999), which reduces the amount of Cu^{+} in the solution of click reaction as well as reduces its catalytic ability. On the other hand, copper (I)-catalyzed click reaction is unfavorable in alkaline condition (pH > 10) because the metal hydroxides formed by Cu^{2+} and Cu^{+} hamper the catalytic activity of Cu^{+}. Accordingly, Tris–HCl buffer at pH 7.4 was exploited in our experiment.

Sodium ascorbate was used as a reductant to generate Cu^{+}, the catalyst in CuAAC, through the reduction of the Cu^{2+}. The sufficient amount of Na-Asc provides a reducing environment which is favorable for high yield of Cu^{+}. For optimization of Na-Asc concentration, different concentrations of Na-Asc, varying from 20 μM to 2 mM, were added to the click reaction solution and the efficiency of click reaction was investigated by measuring the fluorescence signal of the sensor. As illustrated in Fig. S8, the increasing concentration of Na-Asc from 0 μM to 500 μM induced a sharp increase of fluorescence signal and a plateau was obtained above 500 μM Na-Asc. Hence, Na-Asc was optimized to be 500 μM in this sensing system.

After the click ligation and toehold-displacement, the resulting reaction mixture was incubated with K^{+} to implement the formation of stable intra-molecular G-quadruplex because K^{+} is considered as an efficient G-quadruplex stabilizer (Kong et al., 2009a). Hence, the influence of different concentrations of K^{+} on the sensing system was measured. As shown in Fig. S9, with the increasing concentration of K^{+}, the fluorescence signal (F/F_0) apparently increased (0–20 mM K^{+}) and reached the maximum at 20 mM K^{+}, then turning to a slight decrease (20–100 mM K^{+}). Consequently, 20 mM K^{+} was chosen in this study.

3.4. Sensitivity and selectivity of the Cu^{2+} biosensor

Under the optimized conditions, the fluorescent biosensor was applied to detect the copper ion. Different concentrations of Cu^{2+} were added to the click reaction solution and incubated for 90 min at room temperature. After toehold-displacement and CV stain, the fluorescence intensity (FI) of the sensor was measured for quantitative analysis. The fluorescence intensity versus the varying concentration of Cu^{2+}(0–100 μM) was recorded and is illustrated in Fig. 3. When the concentration of Cu^{2+} was between 0 and 50 μM, the FI was enhanced substantially with the increase of Cu^{2+} concentration, indicating that the higher concentrations of Cu^{2+} generated more ligation product of A+B as a consequence. The FI reached a plateau at 50 μM Cu^{2+} partially due to the fact that the click reaction was completed. The linear range is 0.1–3.0 μM and its calibration equation is $FI=693.5625\ C_{Cu}+5141.28$ with a correlation coefficient of 0.998. The detection limit (DL) is determined to be 65 nM ($S/N=3$). This detection limit is much lower than that of previously reported Cu^{2+} assays using conventional click reaction (DL above 1 μM) because of highly efficient DTS (Hua et al., 2012; Song et al., 2010; Sanji et al., 2011; Zhou et al., 2008), but relatively higher than that of CuAAC-based Cu^{2+} assay involving enzymatic amplification (DL=10 nM) (Su et al., 2013). Considering that the proposed method is a proof-of-principle of homogenous fluorescent CuAAC-based assay without signal amplification, it is rational to expect that our DTS-based method can be readily integrated with various nucleic acid amplification for further improvement of its detection limit. Moreover, compared with the previously reported DTS-based biosensors requiring thermal treatment and separation, the established detection method shows more facile detection procedure with lower DL owing to its homogenous fluorogenic strategy (Shen et al., 2012; Xu et al., 2010). The maximum contaminant level of Cu^{2+} in the United States, Canada or the European Union is ~20 μM, 15 μM or 30 μM, respectively. They can be quantitatively detected by the proposed sensor after an easy dilution process.

The high selectivity of CuAAC reaction for copper ion endows the proposed biosensor with excellent selectivity. The control experiments showed that no fluorescence signal was observed for other environmentally relevant metal ions, including Ag^{+}, Ca^{2+}, Cd^{2+}, Co^{2+}, Fe^{2+}, Hg^{2+}, Mn^{2+}, Ni^{2+}, Zn^{2+}, Pb^{2+}, Cr^{3+},

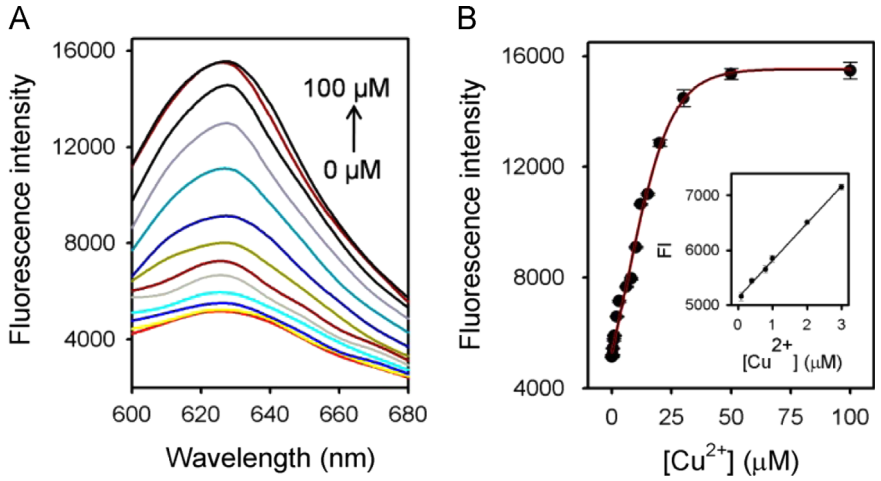

Fig. 3. (A) Typical fluorescence spectral responses of the proposed assay to Cu^{2+} of varying concentrations (0, 0.1, 0.4, 0.8, 1.0, 3.0, 6.0, 10.0, 12.0, 16.0, 20.0, 30.0, 50.0 and 100.0 μM). (B) Fluorescence response at 630 nm of the proposed assay versus Cu^{2+} concentration. Inset: derived calibration curve.

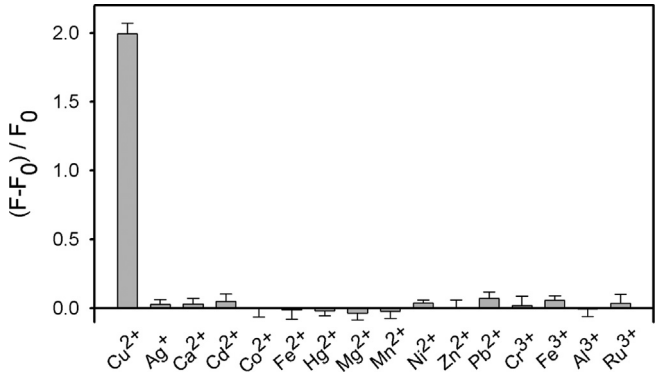

Fig. 4. The selectivity of the Cu^{2+} sensing system. The concentration of Cu^{2+} and the other metal ions were 50 μM.

Fe^{3+}, Al^{3+} and Ru^{3+} at concentration of 50 μM (Fig. 4). It is worth to note that Ru^{3+}, another known metal ion capable of catalyzing alkyne-azide Huisgen cycloaddition, exhibits no interference on our detection system probably due to that Ru^{3+} prefers to implement its catalytic activity in organic medium with the aid of the specific organic ligands (Zhang et al., 2005). Additionally, the coexistence of other metal ions (Ag^{+}, Ca^{2+}, Cd^{2+}, Co^{2+}, Fe^{2+}, Hg^{2+}, Mn^{2+}, Ni^{2+}, Zn^{2+}, Pb^{2+}, Cr^{3+}, Fe^{3+}, Al^{3+} and Ru^{3+} or a mixture of all these metal ions; 50 μM each) suggest a negligible interference for Cu^{2+} assay (Fig. S10). Compared with other sensors for Cu^{2+} ion, the proposed biosensor shows excellent selectivity owing to the high specificity of the alkyne-azide click cycloaddition to the catalysis of copper ions. These results show that our method could be used for detection of Cu^{2+} in complicated real water samples.

3.5. Assay of Cu^{2+} in river water samples

To examine whether the proposed sensing system was feasible to real samples, real and spiked river water samples (Xiangjiang River, Changsha, China) with different concentrations of Cu^{2+} were investigated by the proposed method. The river water samples collected were filtered through a 0.45 μm membrane. Then, the concentration level of Cu^{2+} in river water was evaluated using the proposed method. However, no fluorescence signal was observed for the river water sample using this proposed method. The result indicates that there is no detectable Cu^{2+} in the river water probably due to that the concentration of Cu^{2+} in the river water is less than the detection limit given by our method. Thereby, we added Cu^{2+} with various concentrations to the as-prepared water samples and then employed the proposed method to analyze the spiked river water. The results are summarized in Table S1, the recoveries of standard addition were 95%, 104%, 98%, 104% and 102% for Cu^{2+} ion concentrations of 0.2, 0.5, 1.2, 1.5 and 2.5 μM, respectively, using our fluorescence method. All the results obtained by our method are comparable to those of inductively coupled plasma mass spectrometry (ICP-MS), confirming that the proposed sensing system is applicable for Cu^{2+} assay in real samples.

3.6. Assay of GSH/Cu^{+} using the proposed method

Glutathione (GSH) is the most abundant intracellular non-protein thiol and is present in all living cells in concentrations varying from 1 mM to 6 mM. Glutathione (GSH) can reduce Cu^{2+} to Cu^{+} and form a stable complex GSH/Cu^{+} even in the presence of oxygen (Ciriolo et al., 1990). For this reason, complex of GSH/Cu^{+} may provide a pooling mechanism for Cu^{+} in living cells. Hulme's group demonstrated that GSH/Cu^{+} could be used as the catalyst for the alkyne-azide Huisgen cycloaddition (Viguier and Hulme, 2006). Hence, the proposed method was modified for detection of GSH/Cu^{+} complex. The capacity of GSH/Cu^{+} complex for catalyzing chemical ligation of our probe was proved by denaturing PAGE. As depicted in Fig. 5A, in the presence of GSH/Cu^{+} complex, the click reaction product band A+B was appeared and it became gradually brighter with increasing Cu^{2+} concentration from 5 μM to 200 μM, demonstrating the GSH/Cu^{+} complex as a potent catalyst for click chemistry. Fig. 5B exhibits the fluorescence spectral responses of the DTS-based assay to GSH/Cu^{+} of varying concentrations. The fluorescence intensity monotonically increases with the increase of GSH/Cu^{+} concentration. A calibration curve with a high correlation coefficient (R=0.992) for analyzing the GSH/Cu^{+} was obtained. The linear range of the GSH/Cu^{+}-based method is from 1 μM to 30 μM with a detection limit of 1 μM (S/N=3) (Fig. 5C), which is lower than that of previously reported assays based on conventional click reaction (Song et al., 2010; Viguier and Hulme, 2006). The experimental results suggest that our method has potential for detection of biological copper(I).

4. Conclusions

In summary, we developed a novel turn-on fluorescent sensor for Cu^{2+} by integrating the DNA-templated click reaction and

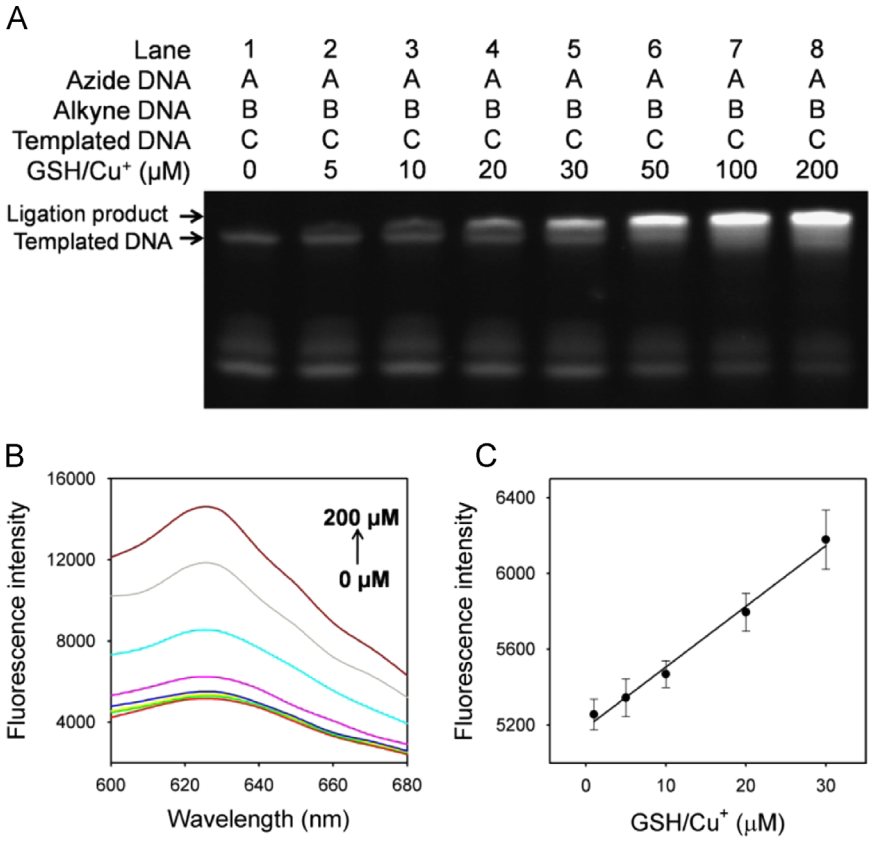

Fig. 5. Fluorescent detection of GSH/Cu^+. (A) Product analysis of click reaction at room temperature for 90 min by denaturing PAGE. (B) Typical fluorescence spectral responses of the DNA ligation assay to GSH/Cu^+ of varying concentrations (0, 1.0, 5.0, 10.0, 20.0, 30.0, 50.0, 100.0 and 200.0 μM, respectively). (C) Fluorescence response at 630 nm of the DNA ligation assay versus varying GSH/Cu^+ concentrations.

G-quadruplex structure switch. In this proof-of-principle work, copper ion detection was achieved by the chemical ligation of split G-quadruplex fragments via DNA-templated CuAAC reaction and the fluorogenic property of CV capable of discriminating the intact intra-molecular G-quadruplex from split one. The high sensitivity and excellent selectivity of this assay attribute to the high yielding capability of DTS and great specificity of click chemistry. Compared with the existing DTS-based biosensors requiring thermal treatment and separation, this approach provides a straightforward and homogenous strategy to achieve "mix-and-read" detection. Additionally, this approach can be further improved by optimizing the G-quadruplex sequence and choosing more specific G-quadruplex fluorogenic probe. Furthermore, this strategy of DTS-mediated ligation of split G-quadruplex can readily introduce various G-quadruplex-related techniques into DTS-based biosensing, such as the peroxidase-mimic DNAzyme. Moreover, this strategy is easily expandable to detect different targets by facilely altering the DNA-encoded reactants. Therefore, this method as a representative demonstrates the great promise of DTS-mediated G-quadruplex formation in biosensors development.

Acknowledgments

This work was financially supported by the National Natural Science Foundation of China (Nos. 21222507, 21175036, 21235002, and 21190044), the Foundation for Innovative Research Groups of NSFC (Grant 21221003), the National Basic Research Program of China (973 Program, Nos. 2009CB421601 and 2011CB911002), the Program for New Century Excellent Talents in University (NCET-10–0366), and the Ph.D. Programs Foundation of the Ministry of Education of China (No. 20120161110025).

Appendix A. Supplementary material

Supplementary data associated with this article can be found in the online version at http://dx.doi.org/10.1016/j.bios.2013.12.019.

References

Arthanari, H., Bolton, P.H., 2001. Chem. Biol. 8, 221–230.
Bhasikuttan, A.C., Mohanty, J., Pal, H., 2007. Angew. Chem. Int. Ed. 46, 9305–9307.
Byrnes, R.W., Antholine, W.E., Petering, D.H., 1992. Free Radic. Biol. Med. 13, 469–478.
Barceloux, D.G., 1999. Clin. Toxicol. 37, 217–230.
Chan, T.R., Hilgraf, R., Sharpless, K.B, Fokin, V.V., 2004. Org. Lett. 6, 2853–2855.
Ciriolo, M.R., Desideri, A., Paci, M., Rotilio, G., 1990. J. Biol. Chem. 265, 11030–11034.
Doyon, J.B., Snyder, T.M., Liu, D.R., 2003. J. Am. Chem. Soc. 125, 12372–12373.
Deiters, A., Cropp, T.A., Mukherji, M., Chin, J.W., Anderson, J.C., Schultz, P.G., 2003. J. Am. Chem. Soc. 125, 11782–11783.
Gartner, Z.J., Tse, B.N., Grubina, R., Doyon, J.B., Snyder, T.M., Liu, D.R., 2004. Science 305, 1601–1605.
Gartner, Z.J., Kanan, M.W., Liu, D.R., 2002. J. Am. Chem. Soc. 124, 10304–10306.
Georgopoulos, P.G., Roy, A., Yonone-Lioy, M.J., Opiekun, R.E., Lioy, P.J., 2001. J. Toxicol. Env. Health-Part B-Crit. Rev. 4, 341–394.
Hurley, L.H., 2002. Nat. Rev. Cancer 2, 188–200.
Halpin, D.R., Harbury, P.B., 2004. PLoS Biol. 2, 1022–1030.
Hua, C., Zhang, W.H., De Almeida, S.R.M., Ciampi, S., Gloria, D., Liu, G.Z., Harper, J.B., Gooding, J.J., 2012. Analyst 137, 82–86.
Kong, D.-M., Ma, Y.-E., Guo, J.-H., Yang, W., Shen, H.-X., 2009a. Anal. Chem. 81, 2678–2684.
Kong, D.-M., Ma, Y.-E., Wu, J., Shen, H.-X., 2009b. Chem. Eur. J. 15, 901–909.
Kanan, M.W., Rozenman, M.M., Sakurai, K., Snyder, T.M., Liu, D.R., 2004. Nature 431, 545–549.
Kleiner, R.E., Dumelin, C.E., Liu, D.R., 2011. Chem. Soc. Rev. 40, 5707–5717.

Kumar, R., El-Sagheer, A., Tumpane, J., Lincoln, P., Wilhelmsson, L.M., Brown, T., 2007. J. Am. Chem. Soc. 129, 6859–6864.
Karsisiotis, A.I., Hessari, N.M., Novellino, E., Spada, G.P., Randazzo, A., da Silva, M.W., 2011. Angew. Chem. Int. Ed. 50, 1–5.
Li, T., Dong, S.J., Wang, E.K., 2010. J. Am. Chem. Soc. 132, 13156–13157.
Leung, C.-H., Chan, D.S.-H., Man, B.Y.-W., Wang, C.-J., Lam, W., Cheng, Y.-C., Fong, W.-F., Hsiao, W.-L.W., Ma, D.-L., 2011. Anal. Chem. 83, 463–466.
Li, X.Y., Liu, D.R., 2004. Angew. Chem. Int. Ed. 43, 4848–4870.
Liu, X.-M., Thaku, A.r., Wang, D., 2007. Biomacromolecules 8, 2653–2658.
Mergny, J.-L., Riou, J.-F., Mailliet, P., Teulade-Fichou, M.P., Gilson, E., 2002. Nucl. Acids Res. 30, 839–865.
Neidle, S., Parkinson, G.N., 2003. Curr. Opin. Struct. Biol. 13, 275–283.
Phan, A.T., Kuryavyi, V.D., Patel, J., 2006. Curr. Opin. Struct. Biol. 16, 288–298.
Que, E.L., Domaille, D.W., Chang, C.J., 2008. Chem. Rev. 108, 1517–1549.
Qiu, S.Y., Gao, S., Zhu, X., Lin, Z.Y., Qiu, B., Chen, G.N., 2011. Analyst 136, 1580–1585.
Rostovtsev, V.V., Green, L.G., Fokin, V.V., Sharpless, K.B., 2002. Angew. Chem. Int. Ed. 41, 2596–2599.
Sen, D., Gilbert, W., 1990. Nature 344, 410–414.
Shen, Q.P., Tang, S.Y., Li, W.H., Nie, Z., Liu, Z.L., Huang, Y., Yao, S.Z., 2012. Chem. Commun. 48, 281–283.
Shen, Q.P., Li, W.H., Tang, S.Y., Hu, Y.F., Nie, Z., Huang, Y., Yao, S.Z., 2013. Biosens. Bioelectron. 41, 663–668.
Song, Y.J., Qu, K.G., Xu, C., Ren, J.S., Qu, X.G., 2010. Chem. Commun. 46, 6572–6574.
Sanji, T., Nakamura, M., Tanaka, M., 2011. Tetrahedron Lett. 52, 3283–3286.
Su, J., Xu, J., Chen, Y., Xiang, Y., Yuan, R., Chai, Y.Q., 2013. Biosens. Bioelectron. 45, 219–222.
Tse, B.N., Snyder, T.M., Shen, Y.H., Liu, D.R., 2008. J. Am. Chem. Soc. 130, 15611–15626.
Viguier, R.F.H., Hulme, A.N., 2006. J. Am. Chem. Soc. 128, 11370–11371.
Wang, Q., Chan, T.R., Hilgraf, R., Fokin, V.V., Sharpless, K.B., Finn, M.G., 2003. J. Am. Chem. Soc. 125, 3192–3193.
Xu, Y., Suzuki, Y., Komiyama, M., 2009. Angew. Chem. Int. Ed. 48, 3281–3284.
Xu, X.Y., Daniel, W.L., Wei, W., Mirkin, C.A., 2010. Small 6, 623–626.
Zhou, Y., Wang, S.X., Zhang, K., Jiang, X.Y., 2008. Angew. Chem. Int. Ed. 47, 7454–7456.
Zhang, L., Chen, X.G., Xue, P., Sun, H.H.Y., Williams, I.D., Sharpless, K.B., Fokin, V.V., Jia, G.C., 2005. J. Am. Chem. Soc. 127, 15998–15999.